



Energy Frontier Research in  
Extreme Environments Center

CARNEGIE  
INSTITUTION FOR  
SCIENCE



# Year Six Annual Progress Report

April 30, 2015



Russell J. Hemley, *Director*  
Timothy Strobel, *Associate Director*  
Stephen Gramsch, *Coordinator*



CARNEGIE  
INSTITUTION FOR  
SCIENCE

# 1. OVERVIEW

## Energy Materials and Extreme Conditions

Investigations on matter in extreme conditions provide critical information for understanding the fundamental basis for materials performance, toward optimization of materials for energy systems, particularly those operating in extreme conditions. In addition, controlling pressure and temperature allows access to energy states and landscapes that can lead to stable compounds and phases not accessible at ambient conditions. This information can be applied to the design of processes whereby these materials may be recovered, synthesized by other routes, or different compositions formed at ambient conditions with the same or even superior properties

## Energy Frontier Research in Extreme Environments (EFree)

**Mission:** *To accelerate the discovery of new energy materials using extreme conditions*

Studies of materials under extreme conditions provide fundamental information in the area of (1) Structural Materials, (2) Energy Conversion and (3) Energy Transport (Fig. 1). Within these focus areas, EFree currently has five *Projects*, as described below. These are managed by *Project Leads* and supported by *Technical Coordinators*.

Our five Projects are actively managed through interactive communication across EFree. Weekly Management Committee meetings are used to discuss day-to-day matters of the Center, while monthly Executive Committee meetings serve as a forum for issues that affect the ongoing research program and the coordination of efforts across the Center as well as at user facilities such as APS, SNS and NSLS. Executive Committee meetings are also used to conduct six-month reviews of all Projects. Highlight presentations *via* videoconferencing, begun in the first phase of EFree, allow the entire Center to meet on a frequent basis and share in the progress of ongoing research. Project meetings are held as needed to gather all participants working on a given Project to share ideas and establish future directions.

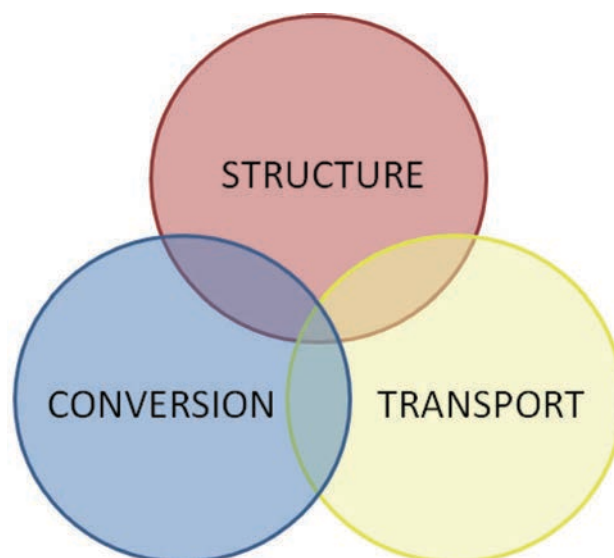


**Figure 1.** Understanding the relationship between different types of materials and their properties at the fundamental level provides information for optimizing materials performance and is a key goal of EFree.

### Management

Russell Hemley, *Director*

Timothy Strobel, *Associate Director*

Stephen Gramsch, *Coordinator*

Morgan Phillips Hoople, *Administrator*

### University Partners

John Badding, *Pennsylvania State University*

Vincent Crespi, *Pennsylvania State University*

Nasim Alem, *Pennsylvania State University*

Brent Fultz, *California Institute of Technology*

Kai Landskron, *Lehigh University*

Roald Hoffmann, *Cornell University*

Neil Ashcroft, *Cornell University*

P. Craig Taylor, *Colorado School of Mines*

### Technical Coordinators

Reinhard Boehler, *High P-T Device Development (Half-Time Carnegie/Spallation Neutron Source)*

DuckYoung Kim, *Theory and Computation (Located at Carnegie)*

Maria Baldini, *Synchrotron X-Ray Techniques (Located at the Advanced Photon Source)*

Chen Li, *Neutron Scattering Techniques (Located at the Spallation Neutron Source)*

## 2. HIGHLIGHTS IN YEAR 6

We summarize key highlights from each of the five EFree projects in terms of progress toward overall project goals as well as research collaborations and synergy across the Center.

### Project 1: *New Nanophase Carbons*

**John Badding, Lead**

**Goal:** *To stabilize and characterize new forms of carbon through tailored synthetic processes for the development of new structural materials*

**Carbon Nanothreads from Compressed Benzene** – In Year 6, a major step forward was realized with the report of the synthesis and characterization of diamond nanothreads<sup>1</sup> in the **Badding** group at **Penn State**. These one-dimensional threads (Fig. 2) contain the smallest identifiable unit of the diamond structure as the repeating motif, and are formed by the slow compression and decompression of benzene.

The material was synthesized using the Paris-Edinburgh press at **SNS** and characterized at Penn State. Theoretical work carried out at Penn State and in the **Hoffmann/Ashcroft** group at **Cornell**, along with further characterization at **Carnegie**, **APS** and **SNS**, have indicated that the nanothreads should have extraordinary properties, including strength and stiffness greater than that of carbon nanotubes and polymer fibers.

**Fullerene-Graphene Composite** – Another research highlight in Year 6 is provided by the finding of remarkable properties at high pressure in a fullerene-graphite composite. In a collaboration between **Carnegie** and **APS**, high pressure experiments using recently-developed, *in-situ* characterization techniques,<sup>2</sup> the material was found to exhibit high strength, high volume compression, superelastic recovery from large volume deformation (~40% volume reduction), high uniaxial strain (up to 6% strain compared with that of a shape memory alloy), and a pressure-induced variable (zero or even negative) Poisson's ratio. This particular

result illustrates the Center-wide synergy that we have built in to our program by having an EFree technical coordinator at APS dedicated to the application of new and emerging synchrotron x-ray methods to ongoing EFree research projects.

### Project 2: *Next Generation Mesoporous Materials* **Kai Landskron, Lead**

**Goal:** *To obtain mesoporous and mesostructured crystalline materials through templated synthetic routes at high pressure for catalysis and related applications.*

**Mesoporous Stishovite** – In the **Landskron** group at **Lehigh**, in collaboration with **Carnegie**, the first synthesis of weakly mesoporous stishovite at 9 GPa and low temperature (500 °C), from a periodic mesostructured FDU-12/carbon composite

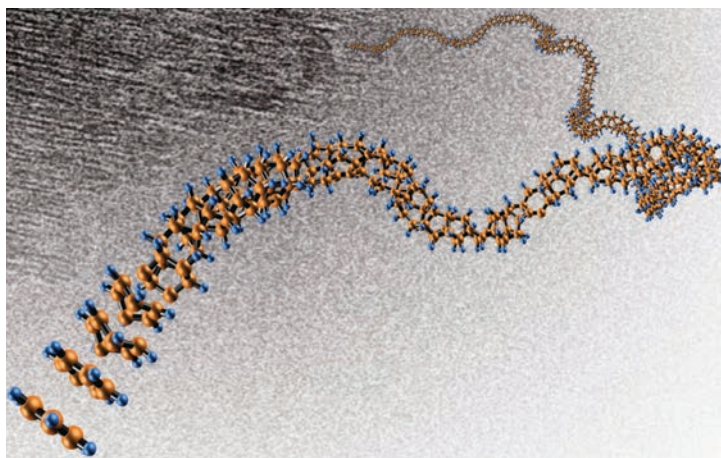


**Figure 2.** Proposed structure of carbon nanothreads from theoretical modeling. The background shows a TEM image of the material indicating crystalline order transverse to the nanothread direction.

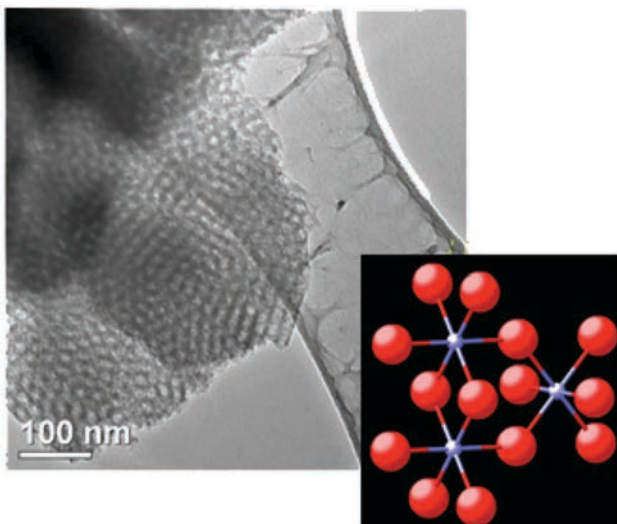


**Figure 3.** Mesostructured stishovite recovered from 9 GPa and 500 °C after plasma etching treatment. Inset: Octahedral 3D coordination in stishovite. Blue spheres, silicon; red spheres, oxygen.



precursor using a multi-anvil apparatus has been accomplished.<sup>3</sup> Mesoporous stishovite (Fig. 3) represents a new class of strong, stable, framework porous materials for catalysis, transport, thermal management and sequestration or adsorption of species from complex aqueous fluids. The **Fultz** group at **Caltech** is beginning to investigate the gas adsorption properties of these materials.

### **Project 3: New Solar Materials (Timothy Strobel, Lead)**

**Goal: To synthesize new materials that will have transformative effects on solar light absorption, conversion efficiencies and manufacturing costs**

**Open-Framework Allotrope of Silicon** – In Year 6, the **Strobel** group at **Carnegie** succeeded in synthesizing the precursor compound  $\text{Na}_4\text{Si}_{24}$  at high pressure and temperature, recovering it to ambient conditions, and de-intercalating the Na under vacuum, to yield  $\text{Si}_{24}$  at ambient conditions.<sup>4</sup> The kinetically stabilized  $\text{Si}_{24}$  has a quasidirect band gap of 1.3 eV, allowing for improved light absorption in the spectral region associated with maximum solar conversion efficiency. Efforts to optimize the synthesis of  $\text{Si}_{24}$  and producing single crystals for the precise measurement of optoelectronic properties are currently underway in collaboration with the **Taylor** group at the **Colorado School of Mines**, which also involves exploring the synthesis of quantum-confined silicon nanoparticles that have optical gaps matched with the solar spectrum and exhibit multiple exciton generation.

### **Project 4: Ion Transport Processes**

**Brent Fultz, Lead**

**Goal: To characterize the structural factors that underlie ion transport in battery materials.**

**Volume for Polaron Hopping in  $\text{Li}_x\text{FePO}_4$**  – Using synchrotron beam time at **APS/HPCAT**, the **Fultz** group at Caltech completed a comprehensive study of the activation volume for polaron hopping in  $\text{Li}_x\text{FePO}_4$  (Fig. 4). For this material,  $V_a = +6 \text{ \AA}^3$ , which is characteristic of Li ion diffusivity, and suggests correlated dynamics of the ions and polarons.<sup>5</sup> This result extends the traditional physics of polarons to include coupling between a polaron and a quasiparticle, and uncovers a new physical process that has only been hinted at in the literature, but in fact is essential to understanding the electrochemical performance of  $\text{Li}_x\text{FePO}_4$ . A collaboration with the **Carnegie** group on first-principles theoretical calculations designed to understand the energetics of these processes is underway.

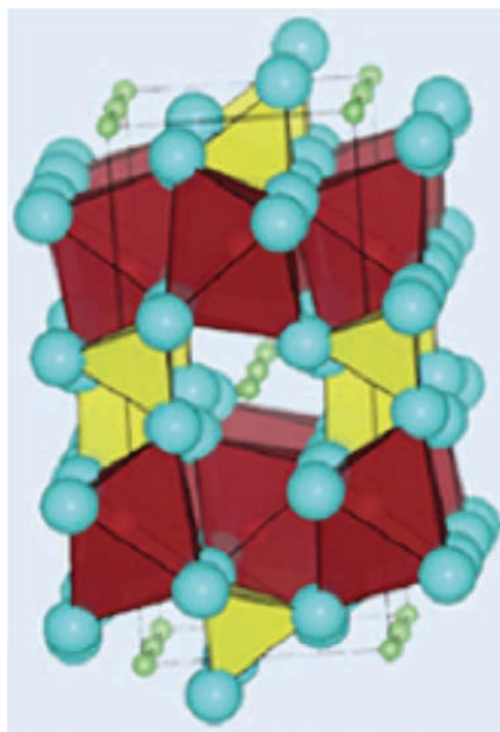


**Figure 4.** Crystal structure of  $\text{Li}_x\text{FePO}_4$ . Red polyhedra,  $\text{FeO}_6$  octahedra; yellow polyhedra,  $\text{PO}_4$  tetrahedra; blue spheres, mobile  $\text{Li}^+$  ions.

### **Project 5: Novel Electron Transport in Hydrogen-Rich Materials (Russell Hemley, Lead)**

**Goal: To uncover novel electron transport properties in hydrogen-rich materials for enhanced electrical transport.**

**Graphene-Like Hydrogen at High Pressure** – With both quantum chemical as well as solid-state physics approaches, the **Carnegie** group has shown that at high pressure, the graphene-like structure of hydrogen at high pressure results from the inherent stability of the six-membered rings, in the same way that benzene is stabilized by aromaticity.<sup>6</sup> Hydrogen is predicted to transform at high pressure to a poorly conducting, graphite-like metal rather than a conventional metal. Ongoing collaborations with the **Cornell** group focus on insulator-metal transitions and related phenomena in simple elemental and molecular systems.



### 3. PROGRESS IN YEAR 6

The main theme of EFree is the synthesis of fundamentally new materials and applying these materials for energy science through development of kinetically stabilized routes to ambient pressure. EFree focuses on studying, manipulating and ultimately controlling materials in regimes outside their fields of thermodynamic stability. We develop and employ new methodological approaches that allow access to new regions of phase space by treating recoverable high-pressure compounds as precursors for subsequent ambient-pressure manipulation. We also exploit pressure to mediate kinetically controlled synthesis of new materials in the solid state. Alternative reaction pathways are ‘engineered’ by using pressure to control the structure of precursors. In many systems, these pathways need not lead to thermodynamically stable reaction products, but to other new materials that can be stabilized by exploiting the kinetic limits of reaction rates. Finally, we use chemical pressure and epitaxial growth to enhance the ambient pressure stability of materials that exhibit exceptional high-pressure energy transport properties.

#### 5.1 NEW NANOPHASE CARBONS

**Synthesis and Characterization of Diamond Nanothreads** – A primary focus in the *Nanophase Carbons* project has been on characterizing the structure of  $sp^3$ -bonded carbon nanothreads that are synthesized under high pressure from benzene.<sup>1,7</sup> At the close of Year 5, we discovered that a solid, crystalline material is formed by high pressure reaction of molecular benzene at 20 GPa upon slow compression and decompression in a Paris-Edinburgh press; images collected with transmission electron microscopy were characteristic of nanothreads (Fig. 2) This work represents a significant advance towards the overall EFree goal of learning to use kinetically controlled reaction chemistry to make nanostructured materials with revolutionary properties

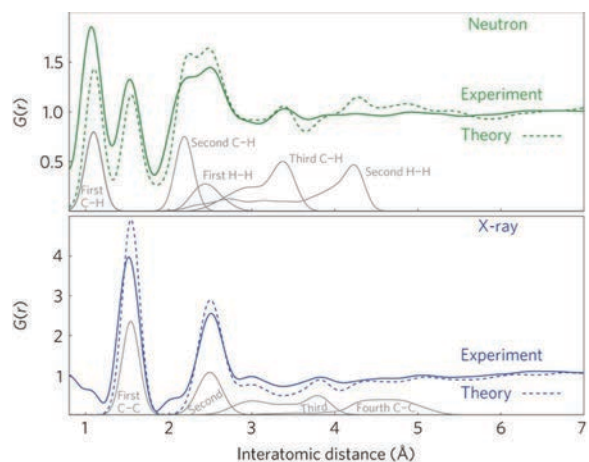


**Figure 5.** Experimental pair distribution function (PDF) and modeled PDF for intermediate nanothread structure. Good agreement is observed out to at least the 3rd nearest neighbor shell.

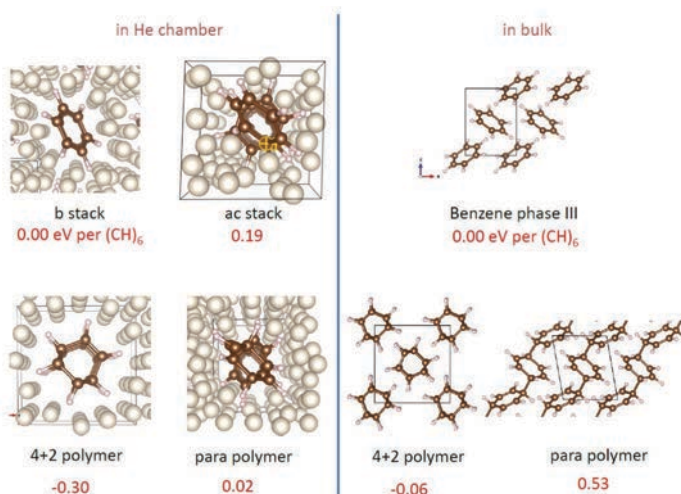


**Figure 6.** At right is a crystal of benzene phase III at 20 GPa, the stacks visible, and below it three-dimensional arrays of model polymers intermediate to nanothread formation. At left, the stacks and polymers are placed in an environment of He atoms acting as a compression medium. The parallel energetics are encouraging for future studies.

useful for energy applications. For example, the strength of these lightweight threads is predicted to be as high or even higher than that of  $sp^2$  bonded carbon nanotubes<sup>8,9</sup> while their unique  $sp^3$  structure may allow for doping to form electronic materials useful for generation and harvesting of light.

Synchrotron x-ray and neutron diffraction studies of the pair distribution function of nanothreads (Fig. 5) have been carried out in Year 6. An intermediate structure formed from candidate nanothread tube (3,0) and polymer I structures by successive Stone-Wales transformations<sup>1</sup> was found to have a predicted pair distribution that best matched experiment. Raman spectroscopic characterization of nanothreads with different isotopic compositions revealed a new C-C "fingerprint" consistent with

calculations of the optical spectrum. NMR spectra exhibited spectral shifts that match those predicted for nanothreads by Maryasin et.al.<sup>10</sup> First principles calculations of the packing and compressibility of nanothreads were also in good agreement with the lattice parameters and shifts in interplanar spacings with pressure determined in diffraction experiments.

**Mechanisms of Nanothread Formation** – In collaboration with the Penn State group, the **Cornell** group is exploring the mechanism of nanothread formation by enumerating one-dimensional intermediate polymers that connect benzene to  $sp^3$  nanothreads. A helium "compression chamber" for benzene stacks and polymers on the way to nanothreads has also been simulated. Figure 6 shows some encouraging parallel energetics in compressed polymer crystals and the model compression chambers. Systematic enumeration of the energetically favorable 1-d  $sp^3$  carbon nanothread structures<sup>11</sup> yields fifty structures that can form from benzene. Fifteen of these are within 80 meV/carbon atom of the most stable structure.

**Exceptional Properties of a Graphene-Fullerene Nanocomposite** – The remarkable properties of the graphene-fullerene nanocomposite described in Section 4 have provided an additional direction within the *Nanophase Carbons* Project. The discovery of fullerene-like spheroids encased in a disordered, multi-layer graphene matrix opens a route for the preparation of new forms of carbon that feature combinations of two or more carbon allotropes. Such combined forms may display properties superior to the properties of either of the components. It is well known that graphene has very high in-plane strength, while fullerene has a large volume deformation capacity, and so the hybrid type-II glassy carbon is expected to have the integrated features of both materials to possess exceptional mechanical properties. Exploration of new synthetic routes and optimized compression-decompression cycles, along with variable composition of fullerene and graphene may be expected to allow tailored topological connectivity to graphene layers and lead to exceptional and tunable mechanical properties, similar to mechanical metamaterials, with a potentially wide range of applications.

**Possible Boron-Substituted Carbon Clathrates** – The creative use of clathrate structures for synthesizing new porous semiconductors at **Carnegie** suggests further theoretical investigations for understanding the stability of various structural alternatives. So far it has proven impossible to make carbon clathrates, as for normal C-C distances, the space inside the polyhedra (see Fig 7. for the Clathrate I structure) is too small for even the smallest guests.<sup>12</sup> At **Cornell**, a theoretical effort is underway along a different direction, which is to negatively charge the clathrate cage by substituting boron for a number of carbons, thereby allowing much smaller  $Be^{2+}$  and  $Li^+$  ions to enter the cage interiors. If the classical clathrate 1 stoichiometry is  $A_8Si_{46}$ , each cage filled, the target composition is for  $Li_8C_{38}B_8$ . There is some precedent, with  $K_7B_7Si_{39}$ .<sup>13</sup> The B substitution will induce larger unit cells, initial explorations will focus on Clathrate VII, with its simpler cages, then subsequently on Clathrate I.

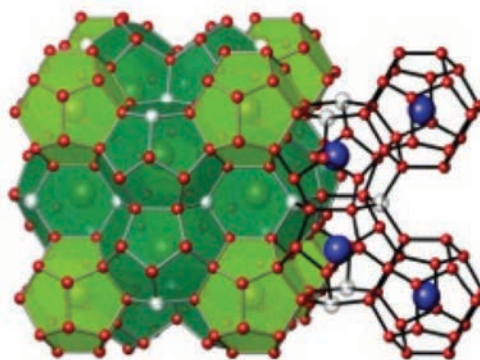


**Figure 7.** Clathrate I structure.

## 5.2 NEXT GENERATION MESOPOROUS MATERIALS

**Synthetic Methods** – A focus of the *Mesoporous Materials* project in Year 6 has been the synthesis of periodic mesoporous carbons at high pressure. Specifically, the **Lehigh** group has investigated the behavior of SBA-15 type soft self-assembled periodic mesoporous carbons.<sup>14</sup> At 21 GPa and 1300 °C transformation into mesoporous diamond occurs. These results show that the formation of mesoporous diamond cannot only be obtained from hard-templated cubic carbon mesostructures, but are also available from soft self-assembled hexagonal mesoporous carbons. This finding significantly simplifies the synthesis of mesoporous diamond because soft self-assembled carbons can be obtained in a single reaction step whereas hard templating requires multiple steps. The soft self-assembled carbons at lower pressure (14 GPa) have also been investigated. In this case, solution-processable diamond nanocrystals form (Fig. 8). The nanocrystal size can be tuned between 50 and 200 nm depending on the reaction time and temperature (1300-1400 °C). Below 14 GPa, no transformation into diamond occurs. Investigations of the behavior of periodic mesoporous carbons at 16 and 18 GPa are also underway. In both cases, phase transformations into diamond have occurred and

more detailed characterization of these materials are ongoing.

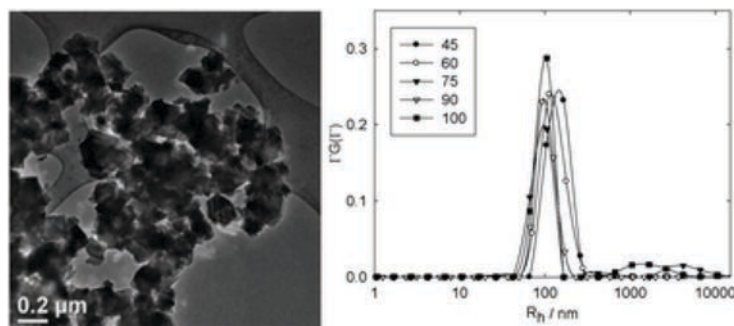


**Figure 8.** TEM image of diamond nanocrystals obtained at 14 GPa and 1300 °C (left) and CONTIN analysis of diamond nanocrystal colloidal solutions (right).

In a collaboration with the **Missouri State** group begun in the first phase of EFree, *in-situ* SAXS measurements were made on periodic mesoporous carbon and silica-based materials as a function of pressure and temperature and in water to supercritical conditions.<sup>15</sup> The data show that periodic mesoporous silica-based materials exhibit substantial mechanical strength. The pore structure, size and related mesoscale properties appear to directly impact the mechanical response of silica-based materials to high pressures and temperatures.

Results indicate that hydrolysis does not seem to be responsible for the mechanical collapse of the pore structure of silica-based mesoporous materials under high pressure conditions. SBA-15 type mesoporous carbon exhibits excellent hydrothermal stability under extreme conditions. The mesostructure of FDU-12 silica is irreversibly disordered after extreme hydrothermal exposure in a manner consistent with H<sub>2</sub>O dissociation reactions causing topological alteration of the silicate network.

In collaboration with **Carnegie**, mesostructured stishovite has been synthesized from a mesostructured FDU-12/carbon composite precursor.<sup>3, 16</sup> Experiments at 14 GPa indicate that a minimum temperature of 500 °C is needed to crystallize stishovite from the amorphous silica precursor with a preserved mesostructure. Transmission electron microscopy combined with small angle x-ray scattering measurements confirm the mesostructure of synthetic stishovite having carbon-filled pores with a diameter of 19 nm, similar to the pore size of the FDU-12 precursor. Calcination of the stishovite/carbon composite at 450 °C in air at ambient condition leads to amorphization of the stishovite. Our results show that mesostructure materials can be synthesized at very high pressures without loss or critical modification of the mesostructure. In a related project, growth of mesoporous quartz single crystals in has been carried out with hydrothermal reactions. Seed plates of quartz single crystals have been incorporated into carbon monoliths. The carbon monoliths have proven stable under hydrothermal conditions at growth temperatures of 350 °C in a temperature gradient of 50 °C.

**Gas Adsorption on Zeolite-Templated Carbons** – In the **Fultz** group at **Caltech**, high-pressure gas adsorption work in has focused on characterizing and understanding the anomalous thermodynamics of gas adsorption on zeolite-templated carbon, a material with a network of nanoscale pores. This work began in the first phase of the Center by looking at methane<sup>17</sup> adsorption on zeolite templated carbon and a number of activated carbons. This has now been expanded to ethane<sup>18</sup> and krypton<sup>19</sup> adsorption, which are potentially important for energy applications. While ethane is the second largest component of natural gas, krypton adsorption is potentially relevant for the development of “closed” nuclear fuel cycles.<sup>20</sup>

Like methane, both ethane and krypton exhibit an anomalous *increasing* isosteric enthalpy of adsorption on zeolite-templated carbon (Fig. 9). This increasing isosteric enthalpy results from the enhancement of lateral intermolecular interactions among the molecules of the adsorbed phase. These enhanced interactions are uniquely promoted by the nanostructured surface of the zeolite-templated carbon, which has a very narrow pore-size

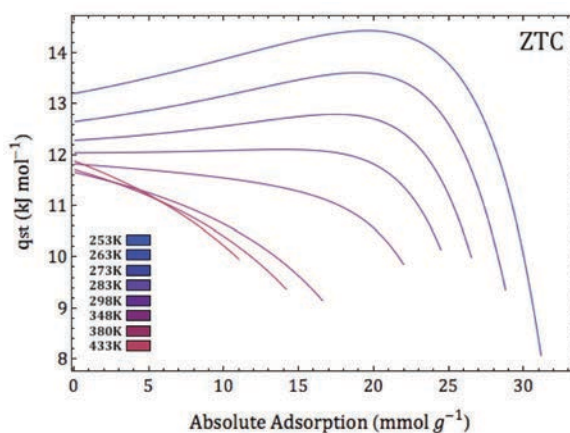


**Figure 9.** The isosteric enthalpy ( $q_{st}$ ) of krypton adsorption on zeolite-templated carbon (ZTC) increases from 13.2 kJ/mol to 14.6 kJ/mol as absolute adsorption increases from 0 to 19.6 mmol/g at 253 K.



distribution centered at 12 Å. Furthermore this work has shown that the increase in isosteric enthalpy roughly scales with fundamental measures of the strength of intermolecular interactions of the individual gases. The resulting increase in the isosteric enthalpy could be helpful for gas storage and separation. These techniques will also be very useful for characterizing the mesoporous materials prepared at **Lehigh** and will provide additional information on their utility for catalytic and fluid adsorption applications.

### 5.3 NEW SOLAR MATERIALS

In the first phase of EFree, a new allotrope of silicon was discovered, with potential to revolutionize solar energy applications.<sup>4</sup> This allotrope, Si<sub>24</sub>, is among the most desirable materials for photovoltaic applications given the earth abundance of silicon and the nature of the quasidirect band gap (~1.3 eV), which leads to

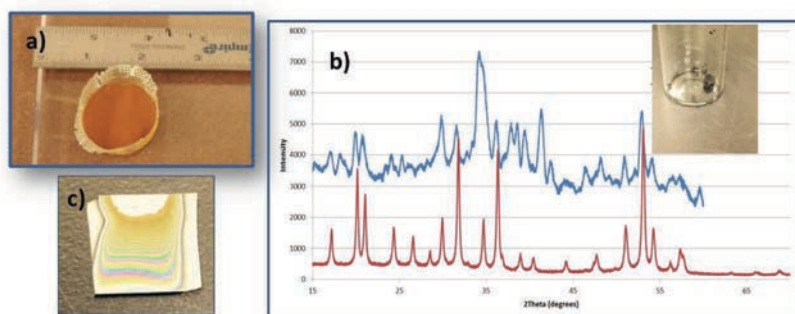


**Figure 10.** (a) Si nanoparticles grown using a standalone PECVD reactor. The particles are deposited on a mesh inside the reactor. (b) Diffraction pattern of the Si clathrates synthesized using Si nanoparticles (blue curve) shown along with the XRD of type II Si clathrate (red curve) synthesized from bulk Si. (c) Si nanoparticle thin film deposited on Si substrate.

significantly enhanced solar light absorption compared with diamond-structured silicon. In addition, the parent clathrate, Na<sub>4</sub>Si<sub>24</sub>,<sup>21</sup> has potential for new advanced battery anodes and gas storage/separation applications. Over the past year in the *Solar Materials* project, the **Carnegie** group has focused on developing robust synthesis methods with the ultimate goal of producing pure single crystals of Na<sub>4</sub>Si<sub>24</sub> and Si<sub>24</sub>. This will enable accurate measurement of physical properties and testing for scaled

synthesis at ambient conditions. Experiments designed to track the structure changes starting from a common diamond structure of Si using a novel two-step methodology have been carried out. Synthesis variables including compositions, pressure, temperature and time have been investigated with the result that nearly-pure (~99 wt%) Na<sub>4</sub>Si<sub>24</sub> has been synthesized. Moreover, methods are under development for optimal sodium removal of the Na from Na<sub>4</sub>Si<sub>24</sub>. Recovered materials with varying sodium composition were sent to our partners at **Penn State** and **Colorado School of Mines (CSM)** for TEM and ESR measurements, respectively. ESR is a useful tool to quantify Na concentration in the Si<sub>24</sub> structure, especially when present in dilute amounts. Other traditional techniques such as diffraction are ineffective at such dilute concentrations. The initial ESR spectra on Si<sub>24</sub> indicate a conduction electron peak due to Na. Further analysis is being conducted to study the charge distribution between Na and Si.

The guest removal from bulk Si clathrates to achieve intrinsic doping levels still remains a challenging task. Si clathrates are generally synthesized from thermal decomposition of a Zintl precursor phase (NaSi),<sup>22</sup> which is synthesized by reacting NaH and Si powder with grain size of several hundred nm. The idea here was to explore if using nanoparticles that are few nm in size as a Si source to synthesize Si clathrate would make guest (Na) removal faster. Si nanoparticles have been synthesized using the PECVD setup at CSM. The Si nanoparticles were reacted with NaH to form NaSi and then underwent thermal decomposition to form Si clathrate. Figure 10 shows the synthesized Si nanoparticles along with the diffraction pattern from post-clathrate formation, indicating that type II Si clathrate was synthesized along with some other impurity phase. Tuning synthesis conditions to obtain phase pure type II clathrate and subsequently study Na removal are underway. Si nanoparticles were also synthesized as a thin film on Si (Fig. 10c) and MgO. If Na removal from Si clathrates synthesized *via* Si the nanoparticle route is faster, then starting from Si nanoparticles in thin film geometry would be useful, especially for optical characterization.

Collaborations with the group at **CSM** have also involved investigations of silicon nanoparticles under pressure. Combining two effects – quantum confinement and multiple exciton generation – silicon nanoparticles in the BC8 structure should have suitable band gaps and will significantly increase the efficiency of solar cells, even beyond the theoretical limit of 33% for a single junction system.<sup>23</sup> Current efforts have focused on the experimental demonstration of this concept. Preliminary work has resulted in the successful transformation of the regular diamond-like Si powder particles (less than 44 μm in diameter) into

the BC8 structure using a metastable back-transformation from high-pressure (Fig.11). The pressure-induced bandgap and photoluminescence manipulations and the phase transitions of the silicon nanoparticles have also been demonstrated.

In addition to silicon, novel allotropes of germanium have also been studied. Mainly due to the difficulty in synthesizing bulk crystalline samples, the band structure of the ST12 Ge is relatively unexplored, but some results indicate that it might have a direct bandgap between 0.6 to 1.4 eV,<sup>24,25</sup> which would make it another good candidate for solar energy conversion. Bulk, ~100% pure Ge ST12 samples with dimension of ~ 2 mm has been synthesized, and the characterization of its optical and electrical properties is actively ongoing.

## 5.4 ION TRANSPORT PROCESSES

In the *Ion Transport Processes* project, the overarching goal is a better fundamental understanding of the transport of both electrons and ions in battery cathode materials. The electronic conductivity mechanism in these materials is small polaron hopping.<sup>26-28</sup> At moderate temperatures, the motion of a polaron quasiparticle is diffusive, and can be understood as an activated process with the jump rate.<sup>29</sup> The effect of pressure on the activation barrier is quantified by the activation volume. The activation volume is expected to reflect the local expansion or contraction in the vicinity of the hopping polaron. A manuscript, published in September of 2014 after much controversy, showed a large suppression of the polaron hopping frequency at elevated pressure in  $\text{Li}_{0.6}\text{FePO}_4$ , indicating an anomalously large activation volume.<sup>5</sup> This large and positive  $V_a$ , more characteristic of ion diffusion,<sup>30</sup> probably results from the correlated dynamics of polarons and mobile Li-ions, a hypothesis that we are testing in ongoing work. Because ion transport is suppressed by pressure, polaronic conductivity should also be suppressed if the polaron-ion interaction energy is large. Although there have been predictions of polaron-ion interactions, this is the first experimental evidence.

Over two beam time runs in July and October 2014 at the **APS**, the **Caltech** group collected a new set of nuclear forward scattering spectra (NFS) of  $\text{Li}_x\text{FePO}_4$  ( $x = 0.4, 0.66, 0.85$ ) at elevated temperatures and pressures. Altering the lithium concentration serves to alter the relative fractions of electron polarons and hole polarons. They are expected to have very different interactions with  $\text{Li}^+$  ions, and different activation volumes (Fig. 12) In February 2015, a new study was carried out on the activation volume for electronic charge hopping in  $\text{Na}_{0.7}\text{FePO}_4$ . The sodium analogue to  $\text{Li}_x\text{FePO}_4$  has recently attracted attention as a promising low-cost cathode material.<sup>31-35</sup> The experimental data seem to show large differences in the dynamics of polaron hopping and differences in the polaron-ion interactions for this material with  $\text{Na}^+$  (instead of  $\text{Li}^+$ ). The size discrepancy between  $\text{Na}^+$  and  $\text{Li}^+$  ions likely affects the activation volume for ion diffusion, and hence polaron hopping. A quantitative comparison of  $E_a$  and  $V_a$  for  $\text{Na}_{0.7}\text{FePO}_4$  to those from the previous study of  $\text{Li}_x\text{FePO}_4$  should show essential differences in the charge dynamics of these two materials.

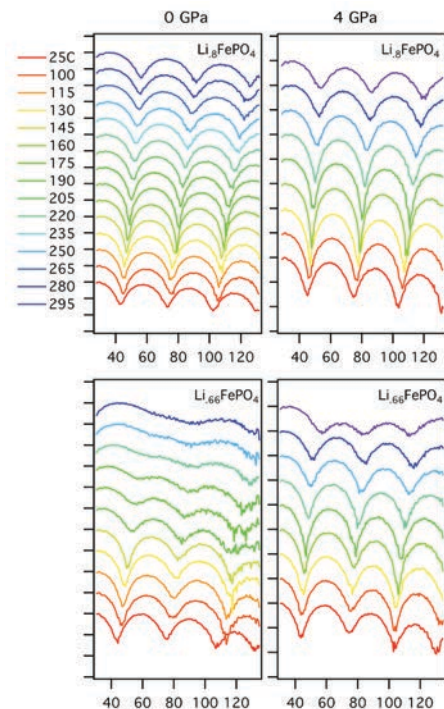


**Figure 12.** Temperature series of NRS spectra in  $\text{Li}_x\text{FePO}_4$  at 0 and 4 GPa. Ambient pressure spectra show large distortions with temperature. Valence fluctuations cause a washing out of the spectral features, a result of a dephasing of the beat pattern from the interference of the nuclear hyperfine levels. At elevated pressure these large spectral distortions occur at higher temperatures. Spectral distortions are much stronger at low lithium concentration.

## 5.5 NOVEL ELECTRON TRANSPORT IN HYDROGEN-RICH MATERIALS

**Hydrogen at Extreme Conditions** – A fundamentally important part of work in the *Hydrogen-Rich Materials*

project is an understanding of hydrogen itself at high pressure and temperature. Theoretical studies at a variety of levels of theory are required to provide input to experimental efforts and lead to useful feedback for tests of theoretical models of high pressure behavior. Ultimately, this synergy can result in an understanding of the behavior of hydrogen-rich materials broadly, and the specific application of structure and bonding models to the isolation of useful materials. In recent work, the **Carnegie** group has approached the hydrogen problem from both the point of view of condensed matter physics as well as quantum chemistry to provide a picture of its behavior at multimegabar pressures.

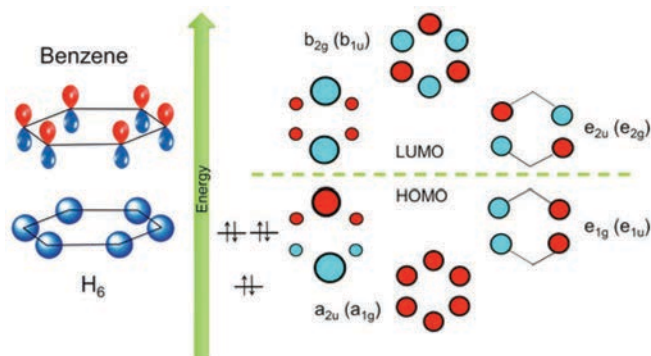


**Figure 13.** Left, correspondence between the  $H\ 1s$ -derived molecular orbitals of the  $H_6$  graphene ring and the  $C\ 2p\ \pi$ -derived molecular orbitals of benzene. Right, closed-shell electronic structure of the graphene-like  $H_6$  ring in hydrogen at high pressure.

At sufficiently high pressure, hydrogen adopts layered structures consisting of graphene-like units, rather than a close-packed solid, which had been assumed for decades. The six-membered ring motif that provides the well-known aromatic stabilization of benzene has a direct parallel in hydrogen (Fig. 13). This stability, which arises from a closed shell of occupied molecular orbitals associated with the  $H_6$  ring, ultimately delays the closing of the band gap, and leads to a metallic state characteristic of a poor, graphite-like metal as opposed to a conventional, atomic metal.<sup>6</sup>

**Metal hydrides of groups 10 and 11** – Gold is one of few elements that does not have an experimentally known hydride in the condensed phase. The **Cornell** group has discovered that no simple binary hydride is likely to be thermodynamically stable, but that there are indications of potentially stable high-pressure alkali metal-stabilized gold hydrides. In related work, ternary alkali metal transition metal hydrides under high-pressure such as  $A_2PdH_2$ , where  $A=Li, Na, K$  have been investigated. Except for  $A=K$ , these compounds are known experimentally at ambient pressure, and are unexpectedly metallic. A new phase is predicted (Fig. 14), and the potential superconductivity of this and other Group 10 and 11 hydrides will be explored.

An enhanced understanding of the behavior of low- $Z$  elements is an essential part of the current project. In the study of the  $Li/Be$  system and the  $Li-Be-B$  ternary diagram begun in the first phase of EFree, there were indications that the ordering of the electronegativity of these elements is modified under high pressure. But it is not easy to define a measure of this useful chemical indicator that carries over to the high-pressure regime. However, a definition of the electronegativity as the average electron binding energy,  $\chi_{CE} = \sum_i \epsilon_i / n$  can be extended to the solid state, and to high-pressure situations. Application of this idea toward understanding theoretical results may provide important insight.

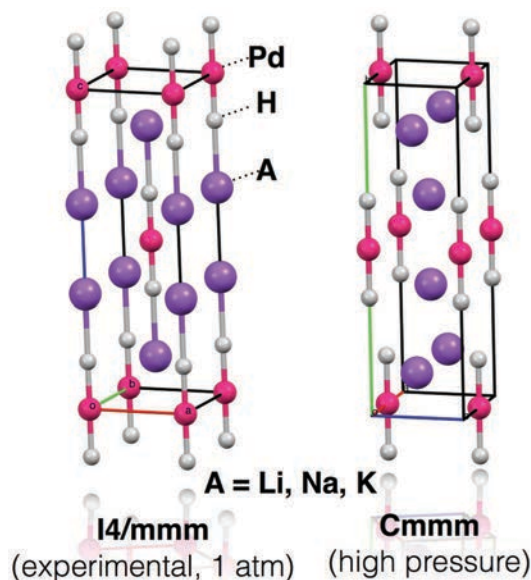


**Figure 14.** The experimental crystal structure of  $A_2PdH_2$ , and the closest in enthalpy predicted high-energy phase, which is thermodynamically preferred above 5, 14 and 100 GPa for  $Li, Na$  and  $K$ , respectively.



## PUBLICATIONS AND OUTREACH

### 11.1 EFree Publications From May1, 2014-April 30, 2015

There were 42 peer-reviewed papers published as a result of EFree funding during the period May1, 2014-April 30, 2015. Citations have been entered at the [energyfrontier.us](http://energyfrontier.us) website.

- 5 papers report scientific results that were supported entirely by EFree.
- 37 papers report scientific results that were jointly supported by EFree and other sources.

### 11.2 EFree Website

The EFree headquarters at Carnegie maintains the EFree website, which is hosted by the Carnegie Institution. A screen shot of the front page of the web site is illustrated in Fig. 15. The website, located at <https://efree.carnegiescience.edu>, contains summaries of current research, descriptions of all ongoing EFree projects, brief biographies of all EFree personnel, personnel news and a cumulative listing of all EFree publications completed since the inception of the Center in 2009. Due to the change in leadership in the second phase of the Center, the EFree website has been completely redesigned, and portions are still under construction.



**Figure 15.** The front page of the EFree website at <https://efree.carnegiescience.edu>

### 11.3 Technology Transfer

Since the inception of the Center in 2009, EFree has had a close working relationship with Washington Diamond. Fundamental investigations into the mechanism of diamond growth by chemical vapor deposition (CVD) have resulted in material that is stronger and tougher than natural diamond or synthetic diamond grown by other methods. Current research focuses on the nature of this enhanced strength and toughness and could broaden the scope of potential applications. CVD diamond produced by Washington Diamond has a variety of scientific and commercial applications, including advanced anvils for extreme conditions experiments, heat sinks for high density, high power electronics, high strength windows for commercial x-ray and IR diagnostics, and semiconductor diamond chips for anticipated optical computing technologies. A slide outlining this development was submitted on January 16, 2015 in response to the request by BES leadership.

## 12. REFERENCES

1. Fitzgibbons, T. C., M. Guthrie, E. S. Xu, V. H. Crespi, S. K. Davidowski, G. D. Cody, N. Alem, and J. V. Badding, Benzene-derived carbon nanothreads, *Nature Mater.* **14**, 43-47 (2015).
2. Zhao, Z., E. F. Wang, H. Yan, Y. Kono, B. Wen, L. Bai, F. Shi, J. Zhang, C. Kenney-Benson, C. Park, Y. Wang, and G. Shen, Nanoarchitected materials composed of fullerene-like spheroids and disordered graphene layers with tunable mechanical properties, *Nature Comm.* **6**, 6212 (2015).
3. Stagno, V., M. Mandal, K. Landskron, and Y. Fei, High-pressure synthesis of mesoporous stishovite: Potential applications in mineral physics, *Phys. Chem. Minerals*, DOI 10.1007/s00269-00015-00739-00268 (2015).
4. Kim, D. Y., S. Stefanoski, O. O. Kurakevych, and T. A. Strobel, Synthesis of an open-framework allotrope of silicon, *Nature Mat.* **14**, 169-173 (2015).
5. Tracy, S. J., L. Mauger, H. J. Tan, Muñoz, Y. M. Xiao, and B. Fultz, Polaron-ion correlations in  $\text{Li}_x\text{FePO}_4$  studied by nuclear resonant scattering at elevated pressure and temperature, *Phys. Rev. B* **90**, 094303 (2014).
6. Naumov, I. I. and R. J. Hemley, Aromaticity, closed-shell effects, and metallization of hydrogen, *Acc. Chem. Res.* **47**, 3551-3559 (2014).
7. Badding, J. V. and V. H. Crespi, Synthesizing carbon nanothreads from Benzene, *SPIE Newsroom*, DOI: 10.1117/1112.1201501.1005713 (2015).
8. Roman, R. E., K. Kwan, and S. W. Cranford, Mechanical properties and defect sensitivity of diamond nanothreads, *Nano Lett.* **15**, 1585-1590 (2015).
9. Stojkovic, D., P. H. Zhang, and V. H. Crespi, Smallest nanotube: Breaking the symmetry of  $\text{sp}(3)$  bonds in tubular geometries, *Phys. Rev. Lett.* **87**, 125502 (2001).
10. Maryasin, B., M. Olbrich, D. Trauner, and C. Ochsenfeld, Calculated nuclear magnetic resonance spectra of polytwistane and related hydrocarbon nanorods, *J. Chem. Theory Comput.* **11**, 1020-1026 (2015).
11. Xu, E. S., P. E. Lammert, and V. H. Crespi, Systematic enumeration of  $\text{sp}^3$  nanothreads, *Nano Lett.*, submitted.
12. Karttunen, A. J., T. F. Fässler, M. Linnolahti, and T. A. Pakkanene, Structural principles of semiconducting group 14 clathrate frameworks, *Inorg. Chem.* **50**, 1733-1742 (2011).
13. Jung, W., J. Lörincz, R. Ramlau, H. Borrmann, Y. Prots, F. Haarmann, W. Schnelle, W. Burkhardt, M. Baitinger, and Y. Grin,  $\text{K}_7\text{B}_7\text{Si}_{39}$ , a borosilicide with the clathrate 1 structure, *Angew. Chem. Int. Ed.* **46**, 6725-6728 (2007).
14. Mandal, M., F. Haso, T. Liu, Y. Fei, and K. Landskron, Size tunable synthesis of solution processable diamond nanocrystals, *Chem. Commun.* **50** (2014).
15. Mayanovic, R. A., H. Yan, A. D. Brandt, Z. Wu, M. Mandal, K. Landskron, and W. A. Bassett, Mechanical and hydrothermal stability of mesoporous materials at extreme conditions, *Micropor. Mesopor. Mater.* **195**, 161-166 (2014).
16. Stagno, V., M. Mandal, W. Yang, C. Ji, H. K. Mao, and K. Landskron, Synthesis of mesostructured stishovite from FDU-12/carbon composite, *Micropor. Mesopor. Mater.* **187**, 145-149 (2014).
17. Stadie, N. P., M. Murialdo, C. C. Ahn, and B. Fultz, Anomalous isosteric enthalpy of adsorption of methane on zeolite-templated carbon, *J. Am. Chem. Soc.* **135**, 990-993 (2013).
18. Murialdo, M., N. P. Stadie, C. C. Ahn, and B. Fultz, Observation and investigation of increasing isosteric heat of adsorption of ethane on zeolite-templated carbon, *J. Phys. Chem. C* **119**, 944-950 (2015).
19. Murialdo, M., N. P. Stadie, N. P. Ahn, and B. Fultz, Krypton adsorption on zeolite-templated carbon and anomalous surface thermodynamics, *Langmuir*, submitted.
20. Ryan, P., O. K. Farha, L. J. Broadbelt, and R. Q. Snurr, Computational screening of metal-organic frameworks for xenon/krypton separation, *Aiche J.* **57**, 1759 (2011).
21. Kurakevych, O. O., T. A. Strobel, D. Y. Kim, T. Muramatsu, and V. V. Struzhkin, Na-Si clathrates are high-pressure phases: A melt-based route to control stoichiometry and properties, *Cryst. Growth Des.* **13**, 303-307 (2013).
22. Kasper, J. S., P. Hagenmüller, Pouchard, and C. Cros, Clathrate structure of silicon  $\text{Na}_8\text{Si}_{46}$  and  $\text{Na}_x\text{Si}_{136}$  ( $x < 11$ ), *Science* **150**, 1713-1714 (1965).
23. Wippermann, S., M. Vörös, D. Rocca, A. Gali, G. Zimanyi, and G. Galli, High-pressure core structures of Si nanoparticles for solar energy conversion, *Phys. Rev. Lett.* **110** (2013).

24. Mujica, A. and R. J. Needs, First-principles calculations of the structural properties, stability, and band structure of complex tetrahedral phases of germanium: ST12 and BC8, *Phys. Rev. B* **48**, 17010 (1993).
25. Malone, B. D. and M. L. Cohen, Electronic structure, equation of state, and lattice dynamics of low-pressure Ge polymorphs, *Phys. Rev. B* **86**, 054101 (2012).
26. Padhi, A. K., K. S. Nanjundaswamy, and J. B. Goodenough, Phospho-olivines as positive-electrode materials for rechargeable lithium batteries, *J. Electrochem. Soc.* **144**, 1188 (1997).
27. Tan, H. J., J. L. Dodd, and B. Fultz, Mössbauer spectrometry study of thermally-activated electronic processes in  $\text{Li}_x\text{FePO}_4$ , *J. Phys. Chem. C* **113**, 2526 (2009).
28. Ellis, B., L. K. Perry, D. H. Ryan, and L. F. Nazar, Small polaron hopping in  $\text{Li}_x\text{FePO}_4$  solid solutions: Coupled lithium-ion and electron mobility, *J. Am. Chem. Soc.* **128**, 11416-11422 (2006).
29. Austin, I. G. and N. F. Mott, Polarons in crystalline and non-crystalline materials, *Adv. Phys.* **18**, 41-102 (1969).
30. Samara, G. A., High-pressure studies of ionic conductivity in solids, *Solid State Phys.* **38**, 1-80 (1984).
31. Moreau, P., D. Guyomard, J. Gaubicher, and F. Boucher, Structure and stability of sodium intercalated phases in olivine  $\text{FePO}_4$ , *Chem. Mater.* **22**, 4126-4128 (2010).
32. Oh, S. M., S. T. Myung, J. Hassoun, B. Scrosati, and Y. K. Sun, Reversible  $\text{NaFePO}_4$  electrode for sodium secondary batteries, *Electrochem. Comm.* **22**, 149-152 (2012).
33. Casas-Cabanas, M., V. V. Roddatis, S. Saurel, P. Kubiak, J. Carretero-González, V. Palomares, P. Serras, and T. Rojo, Crystal chemistry of Na insertion/deinsertion in  $\text{FePO}_4$ - $\text{NaFePO}_4$ , *J. Mater. Chem.* **22**, 17421-17423 (2012).
34. Zhu, Y., Y. Xu, Y. Liu, and C. Luo, Comparison of electrochemical performances of olivine  $\text{NaFePO}_4$  in sodium-ion batteries and olivine  $\text{LiFePO}_4$  in lithium-ion batteries, *Nanoscale* **5**, 780-787 (2012).
35. Lu, J., S. C. Chung, S. I. Nishimura, and A. Yamada, Phase Diagram of Olivine  $\text{Na}_x\text{FePO}_4$  ( $0 < x < 1$ ), *Chem. Mater.* **25**, 4557-4565 (2013).